Wind-induced Swing Response Analysis of Bundled Conductors under Coupling Action of Severe Ice and Wind

Zhang Yuelong[1], Lou Wenjuan[1], Huang Mingfeng[1], Bai Hang[1]

[1] College of Civil Engineering and Architecture, Zhejiang University, China

zhangyuelong@zju.edu.cn, louwj@zju.edu.cn, mfhuang@zju.edu.cn, 306636536@qq.com

Abstract— **A wind-induced conductor swing flashover and tripping accident occurred on a practical 220 kV transmission line with heavy ice accretion in Zhejiang Province, China, resulting in a six-hour-long power outage for approximately 10,000 households and direct economic losses of RMB 3 million. This paper presents a detailed analysis of this high-voltage transmission line swing flashover accident. Swing angle of the suspension insulator string at the moment of the flashover accident was calculated using the rigid rod method recommended by the Chinese standard. It was found that the calculation results were much smaller than the failure swing angle, which exposed the deficiency of the rigid rod method in calculating the swing response of transmission lines under severe ice and wind conditions, and the reasons for this phenomenon were analyzed in detail. According to the icing picture of the practical transmission line, we fabricated sectional rigid model of the heavily iced conductor in a full scale dimension to investigate its aerodynamic characteristic by high frequency force balance technique in the wind tunnel. We proposed an extended rigid rod method for conductors' swing responses under the coupling action of severe ice and wind and verified its applicability for different lines by the finite element method. The extended rigid rod method proposed in this paper can accurately and conveniently calculate the swing response of different transmission lines under the coupling action of severe ice and wind, and it is more beneficial to a large number of engineering applications than the tedious finite element analysis method.**

Keywords— *Transmission line; iced conductor; wind tunnel test; aerodynamic coefficient; wind-induced swing response; extended rigid rod method*

I. Introduction

Wind-induced swing refers to the phenomenon that overhead transmission lines deviate from their vertical position under the action of wind. Excessive swing may cause flashover and line tripping, which will greatly jeopardize the normal operation of the power transmission system and cause huge economic losses. Thus, it is necessary to accurately calculate the wind-induced swing dynamic response of conductors for design applications.

The wind-induced insulator string swing angle was firstly studied based on the results of the Hornisgrinde test project, and an explicit expression for the variation of swing angle with wind speed was given by fitting the statistical test data [1]. Subsequently, the wind-induced swing observations of practical transmission lines were carried out in Japan and some North American countries [2-3].

With the development of computer technology, many scholars have used the finite element method to study the wind-induced conductor swing. Yan et al. [4] conducted a time-domain analysis of the wind-induced transmission line swing response using ABAQUS software. Since the atmospheric turbulence at the height of a conductor is small, the fluctuating part of the wind-induced conductor response can be considered as a small displacement vibration near the swing position under the action of mean wind load [5], which makes the application of the frequency-domain analysis possible. Haddadin et al. [6] and Loredo-Souza et al [7] calculated the wind-induced swing response of transmission conductors using frequency-domain analysis.

In order to calculate the conductor swing response more easily and quickly for engineering applications, many scholars have proposed simplified calculation models, most of which reduce the conductor-insulator string to a static single pendulum model with a rigid rod-mass point [8-10], i.e., the rigid rod method. Many line design codes [11-13] use the rigid rod method to calculate the swing angle of the suspension insulator string and guide the design of the electrical clearance. However, the rigid rod method is limited to the case where the conductor is not covered with ice, and cannot be applied to the lines with heavy ice in mountainous areas.

Combining the swing flashover accident analysis and wind tunnel tests, we proposed an extended rigid rod method for conductors' swing responses under the coupling action of severe ice and wind. The key idea of this extended method was to replace the original static wind load with the equivalent static wind load to consider the dynamic effects of the fluctuating wind. In addition, the gravity of ice and iced conductors' aerodynamic lifts were also considered. Considering that the rigid rod method estimates the gravity of conductors with a relatively large error when the height difference of the conductor hanging point is large, a correction factor λ was introduced for transmission lines with large height differences in mountainous areas. To verify the applicability of the extended rigid rod method for different lines, the average swing angles for different spans, height differences and conductor tensions were calculated by the extended method and the finite element method, respectively, and the results were compared. The extended rigid rod method proposed in this paper can accurately and conveniently calculate the swing response of different transmission lines under the coupling action of severe ice and wind, and it is more beneficial to a large number of engineering applications than the tedious finite element analysis method.

II. Ice accident of a practical HV transmission line

A. The Practical HV Transmission Line

A section of 220 kV transmission line in Zhejiang Province of China has a total length of 1616 m with five spans. The line is running across a mountainous area with an averaged altitude of about 800 m. Towers 1, 5, 6 are tensile towers, while towers 2, 3, 4 are linear towers. Section view of the HV line is shown in Fig. 1. The two-bundled transmission conductor is LGJ-400/35 steel cored aluminium stranded wire with a spacing between sub-conductors of 200 mm, and the bare conductor outer diameter is 26.82 mm.

There are several reservoirs in the vicinity of the HV line, with high humidity year-round and temperatures in the range suitable for icing. Regional micrometeorology is also well suited for icing. Due to the special geographical location and complex meteorological conditions in the region, the year-round low temperature and high humidity make icing very easy to occur and the icing time is long.
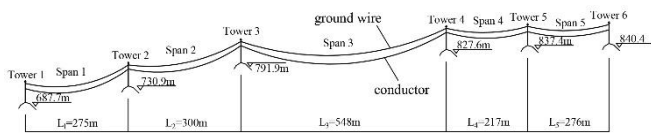

Fig. 1 Section view of a 220kV transmission line in Zhejiang Province.

B. *Fault Summary of the Transmission Line*

From January 23, 2018 to January 30, 2018, influenced by strong cold air, the region where the line is located experienced a cold wave weather process dominated by rainfall and cooling. At 12:00 a.m. on January 29, a wind-induced conductor swing flashover occurred on the transmission line, causing a six-hour-long power outage for about 10,000 households and a direct economic loss of 3 million RMB. Subsequently, on January 30, the line also tripped several times, causing a large and prolonged power outage that greatly affected the normal life of residents. By inspecting the line, obvious flashover traces were found on the tower body and conductor of tower 3. The fault occurred when the fault area does not exist lightning strikes, eliminating the possibility of lightning strikes. According to the surrounding environment and site conditions of the line fault section, combined with the operation and maintenance experience of the HV line, it is preliminarily determined that the local strong convective weather causes the conductor and insulator string to tilt to the side of the tower body, resulting in the minimum air gap between the conductor and the tower body to be insufficient. The flashover traces of the line photographed after ice melted are shown in Fig. 2.

Installed meteorological monitoring equipment was used to record the wind speed, wind azimuth and ice thickness during the flashover accident. It can be calculated that the equivalent ice thickness of each sub-conductor is 36.5 mm at the moment of the line fault, the wind speed at a height of 10 m is 15 m/s, and the angle between the wind direction and the conductor is about 90°. The wind speed component perpendicular to the conductor is very close to the design reference wind speed of 15 m/s for transmission lines in heavily icing areas. By measuring the density of the falling ice, it was determined that the density of the ice on the conductor at this time was approximately 0.7 kg/m³.
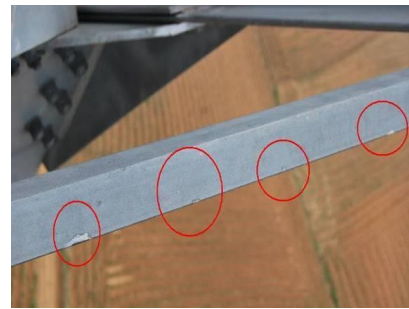

Fig. 2 Photos of the wind-induced swing flashover accident.

C. *Analysis of the Causes of the Flashover Tripping Accident*

1) *Heavying Icing of the Accident Line*

By inspecting the transmission line for wind-induced swing flashover accidents, we found that severe icing occurred on the conductors and that the iced sub-conductors were connected together by many "ice bridges", as shown in Fig. 3. We herein named the iced conductors with this ice shape as a special-shaped iced two-bundled conductor. This ice shape greatly increases the frontal area of the transmission conductor, making its aerodynamic drag coefficient significantly larger, resulting in more pronounced oscillations under wind load and easier flash tripping. According to the surrounding environment and site conditions of the line fault section, combined with the operation and maintenance experience of the HV line, the preliminary judgment is that the HV line is heavily iced so that it has a large swing response under strong winds, making the minimum air gap between the conductor and the tower body is less than the operating requirements.

Fig. 3 Iced conductors of the 220 kV line.

2) *Deficiencies of Wind-induced Swing Analysis Based on the Current Chinese Standard*

The rigid rod method is commonly used in the design of transmission lines [11-13], that is, a single pendulum model to calculate the swing angle of the suspension insulator string, as shown in Fig. 4. The principle of the rigid rod method is static balancing. It treats the suspension insulator string as a rigid rod subjected to uniform load and concentrates the self-weight and the wind load of a conductor on the connection position of the conductor and the suspension insulator string. Swing angle θ can be obtained when the wind load and the self-weight reach static equilibrium. In Fig. 4, G_I and W_I^D are the self-weight of the suspension insulator string and the horizontal wind load it receives, respectively. G_C and W_C^D are the gravity load and horizontal wind load of the conductor, respectively.
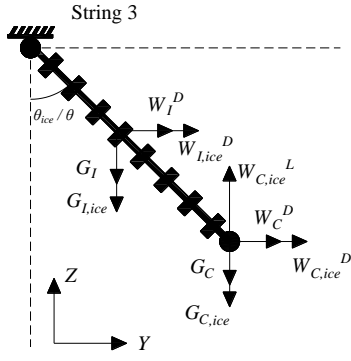
Fig. 4 Rigid rod method for swing analysis.

According to the moment balance relationship, the swing angle θ of the suspension insulator string under wind action can be expressed as:

$$\theta = \tan^{-1}\left(\frac{W_C^D + W_I^D / 2}{G_C + G_I / 2}\right) \tag{1}$$

where W_C^D can be approximately expressed as:

$$W_C^D \approx P_h L_h = P_h \frac{L_1 + L_2}{2} \tag{2}$$

where P_h is the horizontal wind load per unit length of the conductor; L_h is the horizontal span, and its value is equal to the average of L_1 and L_2 (see Fig. 5). G_C can be expressed as:

$$G_C \approx P_v L_v \tag{3}$$

$$L_v = L_h + (\frac{h_1}{L_1} + \frac{h_2}{L_2})\frac{T}{P_v} \tag{4}$$

where P_v is the gravity load per unit length of the conductor; L_v is the vertical span and indicates the horizontal distance between the lowest points of the left and right conductors (see Fig. 5). In Eq. (4), T is the tension of the conductor under the action of wind, which can be solved by iterative method according to the following equation:

$$T - T_0 = \frac{EAL^2}{24}(\frac{P^2}{T^2} - \frac{P_v^2}{T_0^2}) \tag{5}$$

where T_0 is the horizontal tension of the conductor when there is no wind; E is the tensile stiffness of the conductor; A is the cross-sectional area of the conductor; L is the span length; P is the total load per unit length of the conductor when there is wind.

For P_h, the Chinese standard stipulates that the following formula is used for calculation:

$$P_h = \alpha_v \omega_0 \mu_{sc} D \tag{6}$$

where ω_0 is the reference wind pressure; D is the diameter of the wire; α_v is the heterogeneous coefficient of wind pressure along conductor; μ_{sc} the body shape coefficient or the so-called drag coefficient dependent on the shape and dimension of cross-section of the conductor, which is usually determined by wind tunnel test; The current Chinese standard [11] recommends that when $D<17$ mm or the conductor is iced, $\mu_{sc}=1.2$, while $D \geq 17$ mm, $\mu_{sc}=1.1$.

The formula for calculating the wind load on the insulator string is as follows:

$$W_I^D = \omega_0 \mu_{sc} A_j \tag{7}$$

where A_j is the wind area of insulator string.

According to the rigid rod method, the swing angle of the insulator string at the fault tower 3 is 55°. As shown in Fig. 6, when the gap d ($d=\min(d_1, d_2)$) between the conductor and the tower body is less than the critical electrical gap, it will produce a wind-induced swing flashover accident, corresponding to a swing angle of φ_c. For 220 kV lines not exceeding 1000 m above sea level, $d=0.55$ [11]. It can be calculated that the wind-induced conductor swing flashover will occur when the swing angle φ_c of the suspension insulator string reaches 66°.

From the above calculation, it can be seen that the swing angle of the suspension insulator string 3 calculated by the rigid rod method is 55°, which is much smaller than the failure wind swing angle of 66°. For the verification of this flashover accident, it can be seen that the rigid rod method is on the unsafe side when calculating the swing response of a heavily iced line. On the one hand, the rigid rod method is limited to lines without height differences where the conductors are not covered by ice, and cannot be applied to lines with large height differences and heavy ice cover. On the other hand, it ignores the amplifying effect of fluctuating wind loads on the dynamic response.
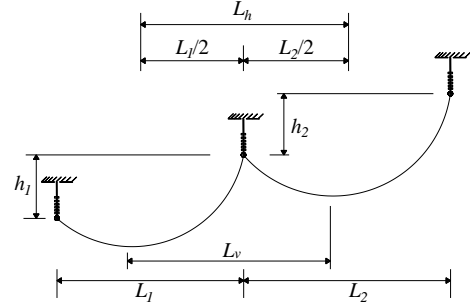

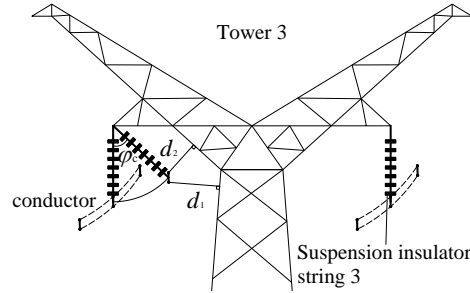Fig. 5 Schematic diagram of the horizontal span L_h and the vertical span L_v.

Fig. 6 Deflection track and the critical swing angle.

III. WIND TUNNEL TESTS FOR HEAVILY ICED CONDUCTORS

D. Test Model of Special-shaped Iced Two-bundled Conductor

According to the icing pictures of the 220 kV HV transmission line (see Fig. 3), the iced sub-conductors were connected together through many "ice bridges" under severe icing conditions. Therefore, in this study, we fabricated sectional rigid model of the special-shaped iced two-bundled conductor in a full scale dimension to investigate its aerodynamic characteristic by high frequency force balance technique in the wind tunnel. The conductor prototype is LGJ-400/35 and its model was made out of ABS plastic in 1:1 ratio with a length of 800 mm [14]. The conductor model's diameter D is 26.82 mm and the distance between the sub-conductor is

200mm. Fig. 7 shows the rigid section model designed according to the practical icing size and its equivalent ice thickness is 36.5mm. Fig. 8 illustrates the cross size of the iced conductor model.
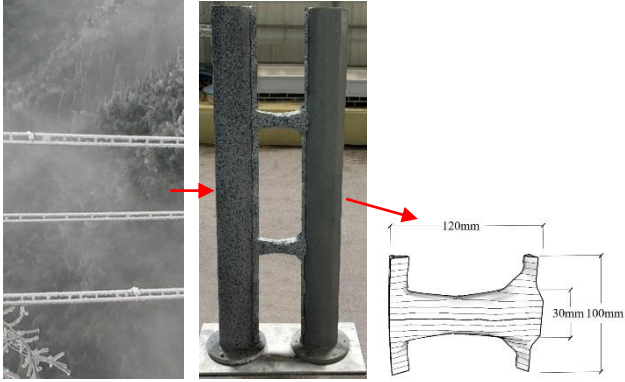

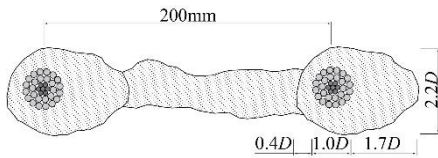Fig. 7 Rigid section model and size of the ice bridge.

Fig. 8 Cross size of the special-shaped iced two-bundled conductor model.

E. Test Facility and Equipment

The test was carried out in the ZD-1 boundary layer wind tunnel laboratory of Zhejiang University. ZD-1 wind tunnel has a closed loop with a working cross section of 4 m (width) × 3 m (height) × 12 m (length), and its wind speed range is 3~55 m/s. High frequency force balance is produced by the German ME-SYSTEM company and used to measure the aerodynamic forces of the special-shaped iced two-bundled conductor. In this test, a homogeneous turbulent wind flow with a 5% turbulence intensity and a mean wind speed of 10m/s was simulated. The conductor model was rigidly connected with the balance through a transfer plate. Since the flow separation at the end of the conductor was eliminated through installing the end plates with smooth surface at the upper and lower ends of the conductor model, the simulated flow around the conductor model could be maintained as two-dimensional flow [15-16], as shown in Fig. 9. A small gap was existed between the model and the top plate to ensure that the wind load on the top plate would not be transferred to the conductor model. In order to eliminate the boundary layer effect of the wind tunnel, we raised up the bottom plate from the ground. The test range of attack angle was 0°~180° with 5° intervals.

F. Aerodynamic Coefficients

Fig. 10 shows the definition of aerodynamic force direction and wind attack angles. Initial ice accretion angle [17] was taken to 0° for iced two-bundled conductors.

The main aerodynamic effects on iced conductors can be expressed in terms of drag, lift forces and torque [18]. In this paper, the results of lift and drag force as well as torque are presented in terms of non-dimensional coefficients as follows:

$$C_L(\alpha) = \frac{\overline{F}_L(\alpha)}{0.5\rho V^2 DH}, C_D(\alpha) = \frac{\overline{F}_D(\alpha)}{0.5\rho V^2 DH}, C_M(\alpha) = \frac{\overline{M}(\alpha)}{0.5\rho V^2 DH} \quad (8)$$

where C_L, C_D and C_M are the average lift, drag and torque coefficients, respectively; F_L, F_D and M are the average value of the measured lift force, drag force and torque respectively; ρ is the air density of 1.225 kg/m³; V is the reference wind speed of 10 m/s; H is the length of the conductor model.

Fig. 11 illustrates the aerodynamic coefficients of the special-shaped iced two-bundled conductor. It can be seen from Fig. 11 that the lift coefficients vary from positive to negative with the change of attack angles, and change in a sinusoidal form. There is only a peak near the attack angles of 25°. Moreover, the drag coefficient curve changes in a half sine wave shape when the attack angle varies from 0° to 180°. The torque coefficient curve peaks near the attack angles of 25°, 60° and 170°.
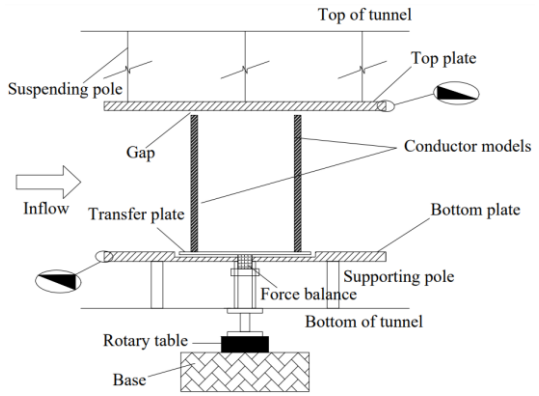
(a) Diagram of devices.

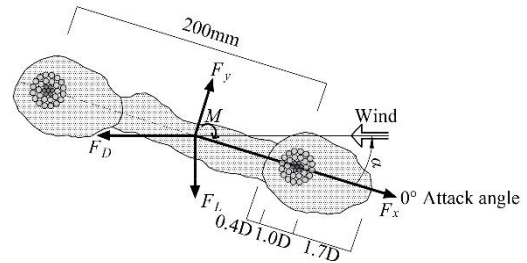(b) Physical picture of devices.

Fig. 9 Wind tunnel test equipment.

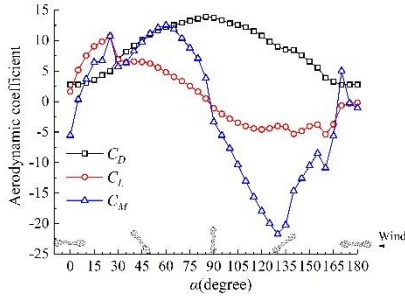Fig. 10 Definition of aerodynamic force direction and wind attack angle α.

Fig. 11 Aerodynamic characteristic of the special-shaped iced two-bundled conductor.

IV. IMPROVEMENT OF THE RIGID ROD METHOD

G. Improved Rigid Rod Method for Swing Analysis

The rigid rod method is used to calculate the swing response of bare conductors and is not suitable for iced conductors. However, the aerodynamic parameters of conductors after icing can change significantly with different ice shapes. Especially under severe ice and wind conditions, the sub-conductors may be covered by ice (see Fig. 3), so that the frontal area increases significantly. These ice shapes will increase the wind-induced swing response of a conductor, posing a serious threat to the safe operation of line. Therefore, we poses an improved calculation method for the swing response of iced conductors. The key idea of this improvement is to replace the original static wind load with the equivalent static wind load to consider the dynamic effects of the fluctuating wind. In addition, the additional gravity and aerodynamic lift generated by ice are also considered. Considering that the rigid rod method estimates the gravity load G_C of conductors with a relatively significant error when the height difference of the hanging point is large, a correction factor λ is required for transmission lines with large height differences in mountainous areas.

The swing angle θ_{ice} calculated by the improved rigid rod method can be expressed as (see Fig. 4):

$$\theta_{ice}=\tan^{-1}\left(\frac{W_{C,ice}^D+W_{I,ice}^D/2}{G_{C,ice}+W_{C,ice}^L+G_{I,ice}/2}\right) \quad (9)$$

where $W_{C,ice}^D$ and $G_{I,ice}^D$ are the equivalent static wind load of the conductor and insulator string under icing condition. $G_{C,ice}$ and $G_{I,ice}$ are the gravity load of the conductor and the suspension insulator string after icing respectively. $W_{C,ice}^L$ is the lift force of the iced conductor.

1) Dynamic Factor β_c Considering the Dynamic Effect of the Wind Load

According to the theory of stochastic vibration, the peak dynamic response of the swing angle of the suspension insulator string (Ω) can be expressed as [4]:

$$\Omega=\bar{\Omega}+K\tilde{\Omega} \quad (10)$$

where $\bar{\Omega}$ is the mean value of the swing angle; $\tilde{\Omega}$ is the root mean square (RMS) of the fluctuating response of the swing angle; K is a statistical peak factor, which is generally set to 2.2 in the Chinese building code.

From Eq. (10), it can be seen that the swing angle response should contain both average and fluctuating parts, while the rigid rod method only considers the average part without considering the amplification effect of fluctuating wind on the

swing response. We herein define a dynamic factor β_c to take into account the dynamic effect of the wind load.

Equivalent static wind load calculation method based on the gust load envelope method (GLE) [19-20] to solve for β_c at node j in the discrete model of the conductor, i.e. $\beta_{c,j}$:

$$\beta_{c,j}=1+2KB_{ri}I_{u,j}(z) \quad (11)$$

$$B_{r_i}=\frac{\sqrt{\sum_{j=1}^{N}\sum_{k=1}^{N}\bar{\beta}_{r_i,j}\bar{\beta}_{r_i,k}\overline{f_jf}_k}}{\sum_{j=1}^{N}\bar{\beta}_{r_i,j}\sigma_{F_j}} \quad (12)$$

where $I_{u,j}(z)$ is the downwind turbulence at the height of node j in the discrete model of the conductor; B_{r_i} is the load discount factor considering the spatial correlation of the fluctuating wind load; $\bar{\beta}_{r_i,j}$ is the influence factor of the fluctuating response in the average wind-induced swing state of the conductor, i.e., the response of node i caused by the unit force acting at node j; $\overline{f_jf}_k$ is the covariance of the fluctuating wind load at nodes j and k; σ_{F_j} is the standard deviation of the wind load at position j; N is the total number of nodes in the model.

$W_{C,ice}^D$ can be calculated according to the discrete point model:

$$W_{C,ice}^D=\sum\beta_{c,j}\bar{F}_j \quad (13)$$

It can be seen that Eq. (13) requires the calculation and summation of $\beta_{c,j}$ and $\bar{F}_j$ at each point of the conductor discrete point model separately, which is not suitable for engineering applications. Considering the small variation of downwind turbulence with the height of the conductor node j, $I_{u,j}$ at the effective height of the conductor can be used as the average $I_{u,j}$ in the whole section to calculate. Eq. (11) can be simplified as:

$$\beta_c=1+2KB_{ri}I_u \quad (14)$$

where I_u is the turbulence at the effective height of the conductor.

B_{ri} is mainly influenced by the line span and does not vary significantly with the basic wind speed and conductor mass. B_{ri} was calculated for different span L [21]. The corresponding calculation model is shown in Fig. 5, and the results are shown in Fig. 12. The fitted calculation equation of B_{ri} was obtained as:

$$B_{ri}=-5\times10^{-10}L_h^3+1.3\times10^{-6}L_h^2-1.2\times10^{-3}L_h+0.92 \quad (15)$$

According to equations (11) to (15), we can obtain:

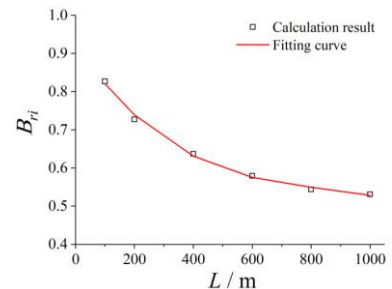$$W_{C,ice}^D=\alpha_v\omega_0\mu_z\beta_cC_DDL_h \quad (16)$$

Fig. 12 Calculation results and fitting curve of B_{ri}.

2) Correction of L_v for Applying to Multi-span Transmission Conductors

In the rigid rod method, from Eqs. (3) and (4), it is obtained that:

$$G_C \approx P_v L_h + \alpha_h T \qquad (17)$$

In which

$$\alpha_h = \frac{h_1}{L_1} + \frac{h_2}{L_2} \qquad (18)$$

Eq. (17) is actually the formula for calculating the vertical tension component at the suspension point when the two ends of the conductor are not equally high. For single span conductors with fixed supports, the Eq. (17) has sufficient calculation accuracy. However, for continuous multi-span conductor, when swing occurs, if the swing angle of the suspension insulator string at both ends of the conductor is different, the height difference between the two ends of the conductor will also change significantly, thus calculating Δh according to the Eq. (18) will cause a large error.

In the mean wind deflection state, the modified α_h (i.e. $\alpha_{h,mod}$) should be expressed as:

$$\alpha_{h,\mathrm{mod}} = \frac{h_1 + \Delta h_1}{L_1} + \frac{h_2 + \Delta h_2}{L_2} = \lambda\left(\frac{h_1}{L_1} + \frac{h_2}{L_2}\right) \qquad (19)$$

where Δh_1 and Δh_2 are the change in height difference between the left and right ends of the conductor, respectively; λ is a correction factor. Based on Eqs. (1) and (17), θ and G_C obtained using the modified α_h are:

$$\theta_{\mathrm{mod}} = \tan^{-1}\left(\frac{W_C^D + W_I^D/2}{G_{C,\mathrm{mod}} + G_I/2}\right) \qquad (20)$$

$$G_{C,\mathrm{mod}} \approx P_v L_h + \alpha_{h,\mathrm{mod}} T = P_v L_h + \lambda \alpha_h T \qquad (21)$$

where θ_{mod} and $G_{C,mod}$ are the modified θ and G_C, respectively. In order to obtain the correction factor λ, the following is obtained through Eqs. (1) and (20):

$$\frac{\tan\theta_{\mathrm{mod}}}{\tan\theta} = \frac{G_I/2 + p_v L_h + \alpha_h T}{G_I/2 + p_v L_h + \lambda \alpha_h T} \qquad (22)$$

Finite element model is established for the accident line as shown in Fig. 14, assuming that the height difference between the suspension points of the two ends of the third span of the conductor are selected as -50 m~20 m respectively, and simulation cases are taken every 10 m. θ_{mod} and θ are the swing angle obtained by finite element simulation and the rigid rod method respectively, and the function relationship between $\tan\theta_{mod}/\tan\theta$ and α_h is fitted to obtain λ=0.74, as shown in Fig. 13. It should be noted that, under the condition of constant basic wind speed, the change of line height difference does not cause a large change in the conductor tension T. Therefore, λ is approximated here as a constant. However, λ is related to the geometric and physical parameters of the conductor and insulator string, especially to the length of the suspension insulator string.

It can be obtained that:

$$G_{C,ice} \approx P_v L_h + 0.74 \cdot \left(\frac{h_1}{L_1} + \frac{h_2}{L_2}\right)T_{ice} + P_{ice} L_h \qquad (23)$$

where P_{ice} is the ice load per unit length of the conductor. T_{ice} is the tension of iced conductor under the action of wind.
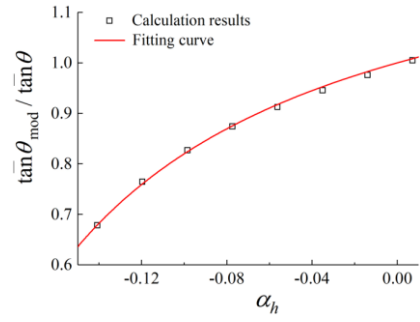

Fig. 13 Calculation results and fitting curve of λ.

3) Swing Angle at the Moment of Flashover Accident Based on Improved Rigid Rod Method

In order to consider the amplification effect of vertical fluctuating wind, a safety factor χ is introduced. When the aerodynamic lift direction is the same as gravity, χ takes 0.9, otherwise χ takes 1.1, as the Chinese Building Load Code [22] also often uses this method to adjust the load [23]. Which is:

$$W_{C,ice}^L = \omega_0 \mu_z C_L D L_h \chi \qquad (24)$$

Using the improved rigid rod method to calculate the swing angle of the suspension insulator string 3 at the moment of the flashover accident, according to the wind tunnel test results in section 3, it is known that the drag coefficient C_D of the iced conductor is taken as 13.73 and the lift coefficient C_L is taken as -1.11. According to the calculation formula in section 4.G.1, β_c=1.3. Thus, the swing angle of the suspension insulator string 3 is 68 ° when the swing flashover occurs based on Eq. (9).

H. Verification of the Improved Method

Based on the aerodynamic coefficients obtained from wind tunnel tests, a refined finite element numerical simulation of the transmission line was carried out to obtain the swing angle of the suspension insulator string 3 under the coupling action of ice and wind. The initial configuration of the conductor under self-weight is a catenary, but the ratio of the sag to the span of the conductor is less than 0.1, so it can be described as a parabola. In the ANSYS modelling process, the conductor can only be pulled, not compressed, so the simulation is performed using LINK10 units. The insulator string is always in tension, and its stiffness is much greater than that of the conductor, so the LINK8 unit is used for simulation. The finite element model of the practical HV transmission line is shown in Fig. 14. Span 5 is the tensile section, which is ignored in the finite element modelling.

The area where the faulty tower is located is identified as the B-type landform according to the Chinese standard, and the average wind speed at each node is obtained based on the exponential law function [22]. In order to reflect the characteristics of near-surface turbulence scale with height, we adopted Kaimal spectrum [24] and considered Davenport spatial correlation [25], and used harmonic superposition method to generate fluctuating wind speed time history at each node.

The time domain method is used to analyze the swing response of the suspension insulator string 3, the unconditionally stable Newmark method is used to directly integrate the nonlinear dynamic equation, and the Newton-Raphson method is used to iterate the displacement at the end

of each time step. Swing angles of the suspension insulator string 3 obtained based on the different methods are listed in Table 1. It can be seen that the differences between the swing angles obtained based on the improved rigid rod method and the time-domain analysis are small, both being greater than failure swing angle φ_c. The results of the rigid rod method calculations provided by the Chinese standard are significantly smaller. It can be concluded that the improved rigid rod method can accurately estimate the swing response calculations for lines with large height differences and heavy ice cover in mountainous areas.

In order to verify the effectiveness of the improved rigid rod method, the average swing angle of the suspension insulator string 3 is calculated by the improved method and the finite element method for different span length, height difference and conductor tension cases of the span 3, and the comparison of the results is shown in Fig. 15. The horizontal coordinate and the vertical coordinate of the figure indicate the calculation result of the finite element method and the improved method, respectively. It can be seen that the improved rigid rod method can achieve high accuracy in calculating the swing angle of iced conductors.

TABLE I. SWING ANGLES OF THE SUSPENSION INSULATOR STRING 3 OBTAINED BASED ON THE DIFFERENT METHODS

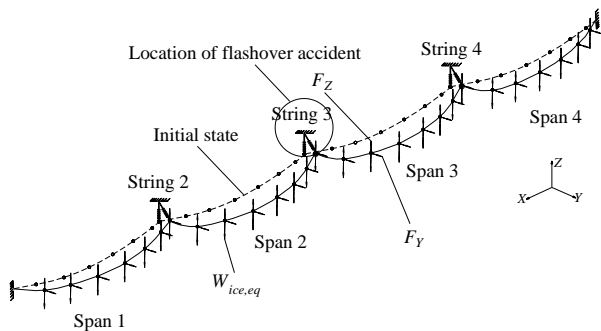| Failure swing angle φ_c	Rigid rod method	Improved rigid rod method	Numerical simulation
66 °	55 °	68 °	67 °

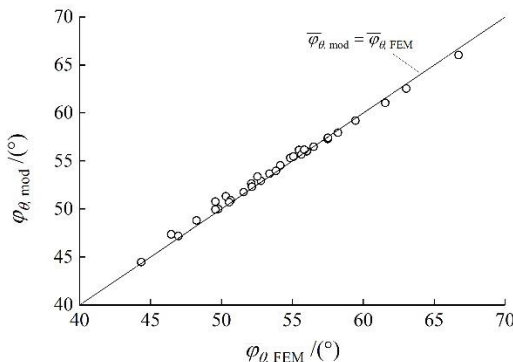Fig. 14 Finite element model of the practical HV transmission line.

Fig. 15 Average swing angles of string 3 by the improved method and the finite element method.

V. CONCLUSIONS

In this paper, a swing flashover accident of a practical transmission line was analyzed, and the aerodynamic coefficients of the iced conductor was obtained through the high frequency force balance wind tunnel test. The rigid rod method provided by the Chinese Standard and the finite element method were used to calculate the swing angle of the line during the flashover accident. An improved rigid rod method was developed for heavily iced conductors in a mountainous area, and its accuracy is verified by finite element simulations. The study concluded as follows:

(1) The occurrence of wind-induced swing flashover accidents on a practical transmission line implies that there are some hidden problems in the calculation of swing response in the Chinese Standard, and transmission lines designed in this way may be on the unsafe side.

(2) For the calculation of wind-induced swing response of lines with large height difference and heavy icing, the rigid rod method is not applicable, and its calculation result is smaller than the practical swing angle. The improved rigid rod method can accurately calculate the swing response of lines under mountainous terrain and severe weather conditions.

REFERENCES

[1] A. R. Hileman. "Weather and its effect on air insulation specifications," *IEEE Trans. Power App. Syst.*, vol. PAS-103, pp. 3104–3116, 1984.

[2] S. Hiratsuka, Y. Matsuzaki, N. Fukuda, et al. "Field test results of a low wind-pressure conductor," *Proceedings of IEEE Region 10 International Conference on. IEEE*, vol.2, pp. 664-668, 2001.

[3] J. G. S. Clair. "Clearance calculations of conductors to buildings," *Transmission and Distribution Conference, IEEE*. pp. 493-498, 1996.

[4] B. Yan, X. Li, L. Wei, et al. "Numerical study on dynamic swing of suspension insulator string in overhead transmission line under wind load," *IEEE Transactions on Power Delivery*, vol. 25(1), pp. 248-259, 2009.

[5] H. A. Oshosha, A. E. Damatty. "Dynamic response of transmission line conductors under downburst and synoptic winds," *Wind & Structures*, vol. 21(2), pp. 241-272, 2015.

[6] S. Haddadin, H. Aboshosha, A. E. Ansary, et al. "Sensitivity of wind induced dynamic response of a transmission line to variations in wind speed,"*Canadian Society of Civil Engineers*, 2016.

[7] A. M. Loredo-Souza, A. G. Davenport. "The effects of high winds on transmission lines," *Journal of Wind Engineering and Industrial Aerodynamics*, vol. 74(98), pp. 987-994, 1998.

[8] K. Tsujimoto, O. Yoshioka, T. Okumura, et al. "Investigation of conductor swinging by wind and its application for design of compact transmission line," *IEEE Transactions on Power Apparatus and Systems*, vol. 11, pp. 4361-4369, 1982.

[9] L. Allen. "Calculation of horizontal displacement of conductors under wind loading toward buildings and other supporting structures," *Papers Presented at the 37th Annual Conference. IEEE*, pp. A1/1-A1/10, 1993.

[10] V. N. Rikh. "Conductor spacings in transmission lines and effect of long spans with steep slopes in hilly terrain," *IE (I) Journal*, vol. 85(5), pp. 8-16, 2004.

[11] Code for design of 1000 kV overhead transmission line: GB 50665-2011[S]. Beijing, China: China Planning Press, 2011.

[12] Technical code for designing of overhead transmission line in medium & heavy icing area: DL/T 5440-2009[S]. Beijing, China: National Energy Administration, 2009.

[13] RUS BULLETIN 1724E-200. Design Manual For High Voltage Transmission Lines[S]. Washington D. C. : U. S. Department of Agriculture, 2005.

[14] R. Alvise, J.Chowdhury, K. Holger, A. Daniel, H. Horia. "Combined effects of wind and atmospheric icing on overhead transmission lines," *J. Wind Eng. Ind. Aerod.*, vol. 204, pp. 104271, 2020.

[15] P.K. Stansby. "The effects of end plates on the base pressure coefficient of a circular cylinder," *Aeronautical J.*, vol. 78 (757), pp. 36-37, 1974.

[16] T.A. Fox, G.S. West. "On the use of end plates with circular cylinders," *Exp. Fluid*, vol. 9(4), pp. 237-239, 1990.

[17] CIGRE. 2005. State of the art of conductor galloping. TB (Technical Brochure), Task Force B2.11.06, December. Convenor, SCB2 WG11.

[18] W.J. Lou, J. Lv, M. F. Huang, L. Yang, and D. Yan. "Aerodynamic force characteristics and galloping analysis of iced bundled conductors," *Wind & Structures*, vol. 18(2), pp. 135-154, 2014.

[19] X. Chen, A. Kareem. "Equivalent static wind loads on buildings: new model," *Journal of Structural Engineering*, vol. 130(10), pp. 1425-1435, 2004.

[20] X. Chen, A. Kareem. "Coupled dynamic analysis and equivalent static wind loads on buildings with three-dimensional modes," *Journal of Structural Engineering*, vol. 131(7), pp. 1071-1082, 2005.

[21] W.J. Lou, G. Luo, W.K. Hu. "Calculation method for equivalent static wind loads and wind load adjustment coefficients for transmission lines," *Journal of Zhejiang University (Engineering Science)*, vol. 50(11), 2016. (in Chinese).

[22] Load code for the design of building structures: GB50009-2012[S]. Beijing, China: China Architecture and Building Press, 2012.

[23] H. Bai. "Wind-induced swing response analysis of transmission lines and simplified calculating method study," *Zhejiang University*, 2021. (in Chinese).

[24] J.C. Kaimal, J.C. Wyngaard, Y. Izumi, et al. "Spectral characteristics of surface-layer turbulence," *Quarterly Journal of the Royal Meteorological Society*, vol. 198(9), pp. 563-589, 1972.

[25] A.G. Davenport. "The dependence of wind load upon meteorological parameters," *Proceedings of the International Research Seminar on Wind Effects on Building and Structure*. Toronto, Canada: University of Toronto Press, pp. 19-82, 1968.